CHEMISTRY
A EUROPEAN JOURNAL

DOI: 10.1002/chem.200701495

Ruthenium Carbene Complexes Bearing an Anionic Carboxylate Chelated to a Hemilabile Ligand

Joseph S. M. Samec and Robert H. Grubbs*[a]

Dedicated to Professor Jan-Erling Bäckvall on the occasion of his 60th birthday

Abstract: A series of bidentate ruthenium-based NHC complexes with the general formula [(H_2IMes)(κ^2-L-COO)ClRu=CHPh)], where L is either PAr_3, HNR_2, or ROR, were prepared from commercially available [(H_2IMes)(PCy_3)Cl_2Ru(CHPh)] (**2**) and the appropriate ligand. The catalytic activities of the complexes were evaluated in ring-closing metathesis reactions. The type of donor ligand has a major impact on both the initiation behavior and also the stability of the complexes. Upon addition of CuCl to the reaction mixture the initiation is improved for the phosphine or amine containing chelates. For the *P,O*-chelate, the fast initiation was followed by decomposition. In the case of the *N,O*-containing chelate, a stable catalytic system was achieved. Trapping experiments support that the nitrogen lone-pair reversibly coordinates CuCl during the reaction.

Keywords: chelates · homogeneous catalysis · metathesis · ruthenium

Introduction

In recent years, olefin metathesis has become a powerful and efficient tool for the formation of carbon–carbon double bonds in organic synthesis and polymer chemistry.[1] The development of well-defined transition-metal complexes as catalysts has been particularly important in expanding the utility of this reaction.[2] Although several catalysts have been reported for olefin-metathesis reactions, ruthenium-based catalysts have received considerable attention because they provide catalytic systems more tolerant to a large number of organic functional groups, moisture, and oxygen. Following the discovery of [(PCy_3)$_2$$Cl_2$Ru=CHPh] (**1**), many researchers have focused on increasing the catalyst activity, selectivity and stability. As identified in previous work, the key to catalyst efficiency is the ratio of the rate of productive olefin metathesis relative to the rate of catalyst decomposition.[3] Furthermore, decomposition products of olefin-metathesis catalysts have been shown to be responsible for unwanted side reactions such as olefin isomerization in addition to loss of activity.[4] The incorporation of *N*-heterocyclic carbene (NHC) ligands in ruthenium catalysts, such as H_2IMes (H_2IMes = 1,3-dimesitylimidazolidine-2-ylidene), has led to the design of catalysts **2**–**4** with

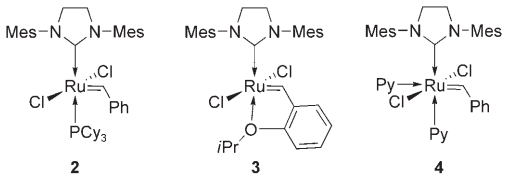

2 **3** **4**

different L-type ligands (L = PAr_3, HNR_2, or ROR) that dissociate from ruthenium during initiation. These catalysts show high activity and fast initiation in a wide range of metathesis reactions.[5]

Despite these advances, the decomposition of the 14-electron methylidene species (H_2IMes)Cl_2Ru=CH_2 (**A**) in catalysis limits the utility of catalysts **2**–**4**, especially with more challenging substrates. Recently, new insights into the decomposition pathways for the Ru-based catalysts have been obtained.[6] For catalyst **2**, it has been established that one decomposition pathway of methylidene **A** involves a nucleophilic attack of free phosphine to generate intermediate **B**

[a] Dr. J. S. M. Samec, Prof. R. H. Grubbs
Division of Chemistry and Chemical Engineering
Arnold and Mabel Beckman Laboratories of Chemical Synthesis
California Institute of Technology
Pasadena, CA 91125 (USA)
Fax: (+1) 626-564-9297
E-mail: rhg@caltech.edu

Supporting information for this article is available on the WWW under http://www.chemeurj.org/ or from the author.

which can then undergo further decomposition (Scheme 1). Very recently, it has been established that catalyst **4** may undergo similar decomposition reactions with pyridine acting as the nucleophile.[6b] As **A** is the critical intermediate in metathesis reactions involving terminal olefins, it would be desirable to stabilize this intermediate without decreasing the rate of productive metathesis.

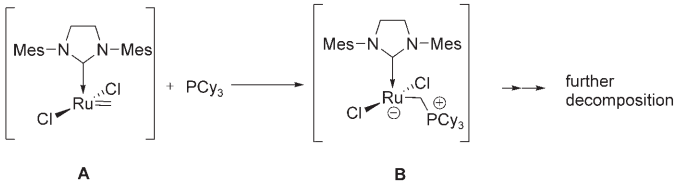

Scheme 1. Decomposition pathway for **A**.

One strategy to prevent the decomposition route outlined in Scheme 1 is to utilize a chelating phosphine ligand, and thereby inhibit the build up of free phosphine. Previously, *N*,*O*-chelates have been reported for NHC-containing analogues **5** and **6**.[7] However, these catalysts require high reaction temperatures and exhibit low metathesis activities.

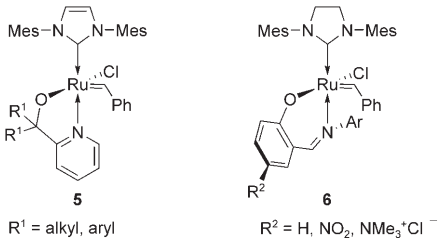

One disadvantage of employing the *N*,*O*-chelates containing Schiff bases is that the preparation involves toxic thallium salts.[8] Recently, we found that replacing the alkoxide with a more electron-withdrawing carboxylate in an *N*,*O*-chelated analogue of catalyst **1** provided a complex with increased rates of reaction.[9,10] Furthermore, the toxic thallium salt could be exchanged for non-toxic and inexpensive Cu_2O. Phosphines, amines, and ethers (such as **2**–**4**, see above) have all been reported as the dissociating L-type ligands for ruthenium-based olefin metathesis catalysts containing an NHC ligand. Therefore chelates based on these functional groups would be of interest, where the L-type ligand never "leaves" the catalyst during the reaction. Herein, we describe non-toxic protocols for the synthesis of a novel series of olefin metathesis catalysts bearing hemilabile L-type ligands, based on *P*-, *N*-, or *O*-tethered to a carboxylate. The reactivity and stability of these catalysts have been studied in ring-closing metathesis (RCM) reactions.

Results and Discussion

Synthesis of complexes 7–9: 2-(Diphenylphosphino)benzoate was chosen as a *P*,*O*-chelate because it is structurally and electronically closely related to triphenyl phosphine, a neutral ligand known to readily dissociate in [(H_2IMes)(PPh_3)Cl_2Ru=CHPh)] (**2′**).[11] Upon addition of **2** to a suspension of the potassium salt of 2-(diphenylphosphino)benzoate in CH_2Cl_2 at room temperature, the desired catalyst [(H_2IMES)(κ(*P*,*O*)(Ph_2P-*o*-C_6H_4COO)ClRu=CHPh] (**7**) is isolated as a red solid in 75% yield after column chromatography (Scheme 2). Catalyst **7** shows characteristic signals in

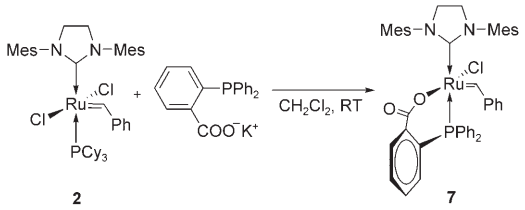

Scheme 2. Synthesis of **7**.

the ^{1}H NMR spectrum at δ 18.97 ppm, which corresponds to the benzylidene proton, in ^{31}P NMR spectrum at δ 32.5 ppm corresponding to the coordinated phosphine, and in ^{13}C NMR spectrum at δ 300.2 ppm (d, $J_{P,C}$ = 9.6 Hz) corresponding to the benzylidene carbon and at δ 169 ppm corresponding to the C=O of the carboxylate group. The carboxylate group is also visible in the IR spectrum at $\nu_{C=O}$ = 1602 cm^{-1}.

Crystals of **7** suitable for X-ray analysis were obtained by slow diffusion of pentane into a solution of benzene at room temperature (Figure 1). In comparison of **2′** and **7**, a significant shortening of the Ru–P bond length from 2.404(3) Å in **2′** to 2.323 (15) Å in **7** is observed. The Ru–O bond length 2.068(3) Å is shorter than the Ru–Cl 2.4016(15) Å. The angle between the carbene carbon of the NHC and P (C-Ru-P) is slightly decreased from 167.1(3) in **2′** to 163.15(16)° for **7**. The angle between the X-type ligands is slightly increased from 166.96(9)° in **2′** to 171.62(10)° for **7** which is in accordance with previously reported *N*,*O*-chelates such as complex **6** (172.50(4)°).[7] All other bond lengths and angles of **7** were similar to those of **2′**.

Proline was chosen as *N*,*O*-chelate because it is commercially available and has previously been used as a chelate with **1**.[9] [(H_2IMes)(L-prolinate)ClRu=CHPh] (**8**) was prepared by the reaction between **2** and the in situ deprotonated L-proline in CH_2Cl_2 at room temperature. Complex **8** was obtained as a mixture of two isomers in 54% yield (Scheme 3). The two isomers are easily separated by column chromatography. The isomer with a higher R_f is the more thermodynamically-stable isomer (**8a**). This isomer shows characteristic signals in the ^{1}H NMR spectrum at δ 19.17 ppm corresponding to the benzylidene, a broad signal at δ 6.59 ppm corresponding to Ar-H of the mesityl group, another broad signal δ 4.10 ppm corresponding to the ethyl-

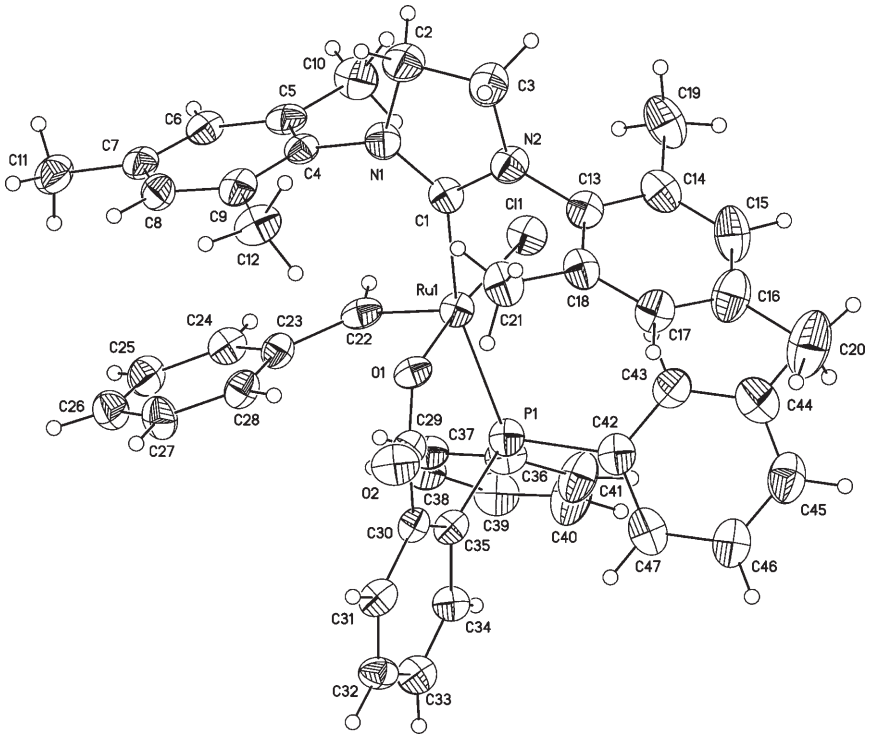

Figure 1. Solid-state structure of **7** with thermal ellipsoids drawn at 50% probability. Selected bond lengths [Å] and angles [°]: Ru1–C22 1.849(6), Ru1–O1 2.068(3), Ru1–C1 2.092(5), Ru1–P1 2.3233(15), Ru1–Cl1 2.4016(15); C22-Ru1-O1 99.7(2), C22-Ru1-P1 93.06(15), O1-Ru1-P1 88.56(10), O1-Ru1-Cl1 171.62(10).

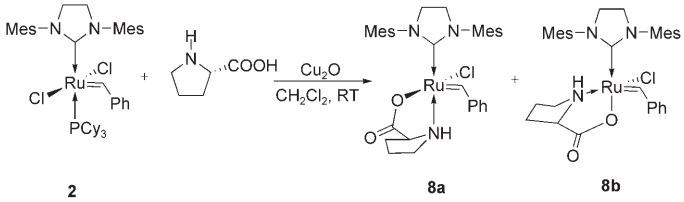

Scheme 3. Synthesis of **8**.

ene bridge in the NHC, and the methyl groups of the mesityl also show up as a broad signal at δ 2.40 ppm. Upon cooling to −10 °C, the broadened signals resolve into individual peaks. In the ^{13}C NMR spectrum the benzylidene carbon signal appears at δ 296.3 ppm, and the C=O of the carboxylate group at δ 183.2 ppm (14 ppm downfield compared with **7**). The carboxylate group is also visible in the IR spectrum at $\nu_{C=O} = 1625\ cm^{-1}$. Only crystals of very poor resolution could be grown of this isomer. Even though it is not possible to get correct bond lengths and angles, the overall structure is evident with the amine moiety of L-proline *trans* to the NHC.

The isomer with the lower R_f, is the kinetically formed isomer (**8b**). This isomer shows characteristic signals in the ^{1}H NMR spectrum at δ 19.03 ppm corresponding to the benzylidene, four separate signals for Ar-H of the mesityl at δ 6.21, 6.52, 7.04, and 7.11 ppm (due to slow rotation of the NHC and the mesityl), and two multiplets at δ 4.16 and 4.08 ppm for the ethylene bridge of NHC, and the methyl residues of the mesityl groups give separate signals between δ 2.01–2.63 ppm. As this kinetically-formed product isomerizes to the thermodynamically more stable product at room temperature, a ^{13}C NMR spectrum was acquired at −20 °C. The benzylidene carbon signal appears at δ 295.3 ppm and the carboxylate at δ 183.0 ppm. The isomerization from **8b** to **8a** results in a 95:5 ratio of **8a**/**8b**. No crystals of **8b** suitable for X-ray crystallography have been grown. As the ^{1}H NMR spectrum reveals inequivalent signals for the protons in the NHC ligand, the kinetic isomer was assigned to have the amine moiety *cis* to the NHC ligand and the carboxylate *trans*. In this configuration, the bulky prolinate hampers the free rotation of the mesityl groups and the NHC ligand. Similar isomers have been observed for amines chelated to the alkylidene used for the design of latent olefin metathesis catalysts.[12]

Tetrahydro-2-furoic acid was chosen as the *O*,*O*-chelate as it is the ether analogue of the successfully anchored proline. Complex **9** was prepared by addition of (*R*)-(+)-tetrahydro-2-furoic acid to a suspension of **2** and Ag_2O in CH_2Cl_2 at room temperature (Scheme 4). The resulting mixture was purified by column chromatography to yield **9** in 81% yield as a green solid in a 10:1 ratio mixture of two isomers. The isomers were not separable by chromatography or crystallization. The major isomer shows characteristic signals in the ^{1}H NMR spectrum at δ 19.00 ppm corresponding to the benzylidene, a singlet at δ 6.80 ppm corresponding to Ar-H of the mesityl group, another singlet δ 3.98 ppm corresponding to the ethylene bridge of the NHC, and the methyl groups of the mesityl groups appear as three separate singlets at 2.19, 2.23, and 2.27 ppm. In the ^{13}C NMR spectrum the benzylidene carbon signal appears at δ 315.6 ppm which is further downfield than the other two complexes, and the C=O of the carboxylate at δ 179.8 ppm, similar to **8**. The carboxylate is also visible in the IR spectrum at $\nu_{C=O} = 1608\ cm^{-1}$.

Activity of complexes 7–9 in RCM: Complexes **7**–**9** were tested for catalytic activity in the ring-closing metathesis (RCM) of diethyl diallylmalonate (**10**) using 1 mol% of catalyst in CD_2Cl_2 and were found to have low activity at 30 °C due to poor initiation. In 10 minutes < 5% conversion was observed for **7**, 10% for **8**,[13] and < 5% for **9**. Analogous non-chelated catalysts containing either *P*-, *N*-, or *O*-based

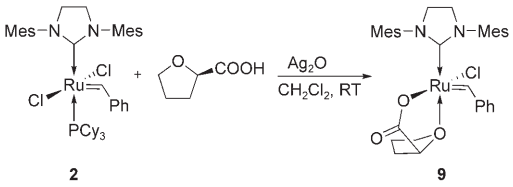

Scheme 4. Synthesis of **9**.

L-type dissociating ligands (see above, **2**–**4**) usually proceed to above 60% conversion under the same reaction conditions.[14] While **7** and **8** continued to perform catalysis, albeit at a low rate, the activity of **9** plateaued at less than 10% conversion. NMR studies indicated fast initiation followed by decomposition. The observation that the *N*,*O*-chelate (**8**) performs better than the *P*,*O*-chelate (**7**) is expected due to the stronger bond between Ru–P and hence a less favored dissociation. However, the low performance of the *O*,*O*-chelate (**9**) was not expected.

A rate enhancement has been reported for catalysts **5** and **6** (see above) at elevated temperatures, therefore the RCM of **10** at 50°C was studied for catalyst **7** and **8**. As expected the rate increased for both **7** and **8**, where **8** is more efficient than **7** (Figure 2). After 110 min, **8** reached above 95% conversion, whereas **7** only reached 60% conversion. The performance of **8** is better than that reported for other *N*,*O*-chelates, which require higher catalyst loadings and longer reaction times.[7c] Interestingly, in the RCM of **10**, first-order kinetics are observed for reactions with catalyst **8**, but not catalyst **7**, indicating that the stability of **7** is not enhanced despite the chelating phosphine. However, the chelate seems to promote stability for **8**.

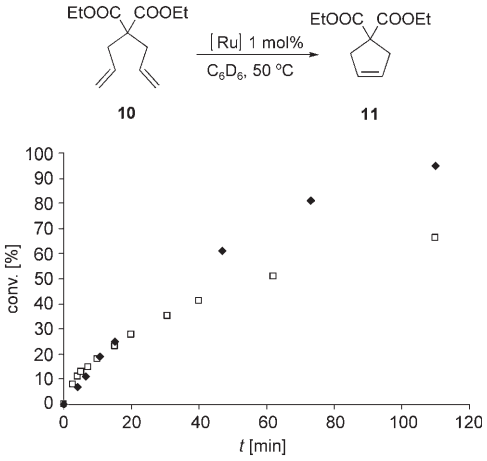

Figure 2. Conversion plot for RCM of 10 with □: **7** and ◆: **8**. The reactions were performed on a 0.08 mmol scale in C_6D_6 (0.75 mL) at 50°C using 1 mol% of catalyst.

Our group previously reported that the metathesis activity of catalyst **1** and **2** could be increased by addition of CuCl.[15] The CuCl is believed to act as a scavenger and activate the catalyst by removing the phosphine ligand from the solution, thereby preventing association of free phosphine to the propagating ruthenium complex. Therefore, we investigated the effect of CuCl on the activity of catalysts **7**–**9**. Indeed, the rate of RCM of **10** was increased for catalyst **7** in the presence of CuCl. The reaction had proceeded to above 95% conversion in less than 10 minutes using 1 mol% of catalyst and 25 mol% of CuCl at 50°C (Figure 3).

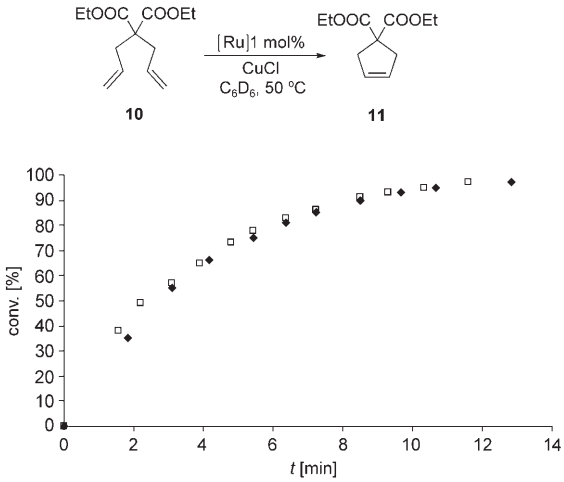

Figure 3. Conversion plot for RCM of **10** with □: **7** and ◆: **8** in the presence of CuCl. The reactions were performed on a 0.08 mmol scale in C_6D_6 (0.75 mL) at 50°C using 1 mol% of catalyst and 25 mol% of CuCl.

There are no reports for the scavenging effect of CuCl for amines in metathesis reactions in the literature. However, the interaction between Cu^I and amino acids has been studied, which prompted us to investigate the effect of CuCl on the activity of **8** in RCM.[16] In less than 10 minutes, the RCM of **10** by catalyst **8** in the presence of CuCl proceeded to above 95% conversion (Figure 3). To our knowledge, this "amine scavenging effect" is not precedent in the literature. A negligible CuCl effect was observed for complex **9** in the RCM of **10**. CuCl may have a lower affinity toward the "harder" oxygen than the "softer" amine or phosphine.

Encouraged by the CuCl effect for catalysts **7** and **8**, a more challenging substrate was chosen. Diethyl allyl methallylmalonate (**12**) forms cyclopentene **13**, featuring a trisubstituted double bond, that is a more demanding reaction than the RCM of **10** due to steric effects. Therefore, substrate **12** better highlights differences in activity and stability. RCM of **12** by catalyst **7** (1 mol%) showed fast initiation in the presence of CuCl, similar to the RCM of **10**, and the reaction reached 50% conversion within 12 minutes (Figure 4). The reaction rate remained constant for three half-lives and the reaction proceeded to 88% conversion within 36 minutes. However, after three half-lives the activity decreased and after 2 h full conversion was not achieved.

RCM of **12** by catalyst **8** (1 mol%) demonstrated the same fast initiation kinetics as observed for catalyst **7** and reached 50% conversion in 13 minutes (Figure 4). Interestingly, catalyst **8** showed higher stability than catalyst **7** and

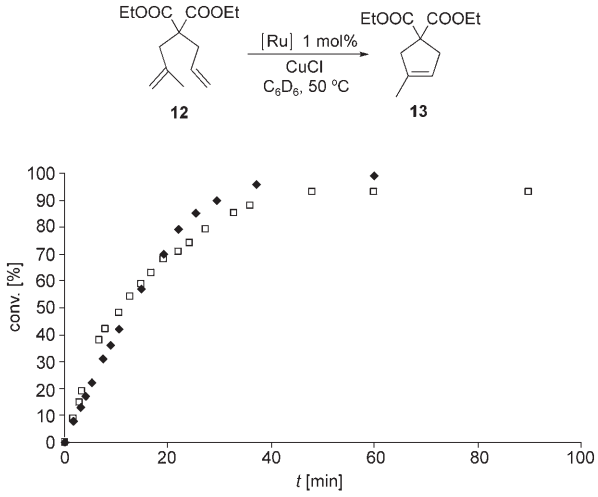

Figure 4. Conversion plot for RCM of **12** with □: **7** and ◆: **8**. The reactions were performed on a 0.08 mmol scale in C_6D_6 (0.75 mL) at 50 °C using 1 mol % of catalyst and 25 mol % of CuCl.

performed the RCM of **12** to above 95 % conversion within 40 minutes without any deviation from first-order kinetics. The reaction proceeded to full conversion within one hour. The RCM of **12** clearly highlights the difference in stability for catalysts **7** and **8**.

Trapping the active intermediate: Because the scavenging effect CuCl is unprecedented for amines, we wanted to study the effect in more detail. The CuCl effect on the activity of complex **8** could be explained by a salt exchange reaction in which the chloride replaces the prolinate ligand to generate the active 14-electron benzylidene species and copper–prolinate (Scheme 5, path A).[17] Alternatively, the CuCl could compete with ruthenium for the lone pair of the nitrogen in the prolinate ligand thereby enabling an open coordination site on ruthenium for the substrate coordination (Scheme 5, path B).

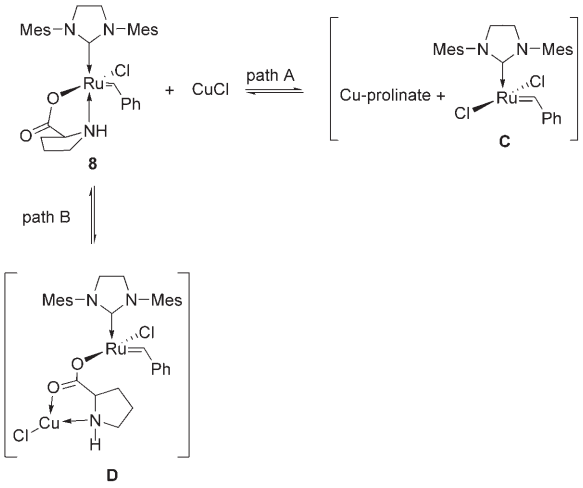

Scheme 5. Mechanism of CuCl activation of **8**.

A way to distinguish between these mechanisms is to trap intermediate **C** or **D** with pyridine. If the 14-electron benzylidene forms, this intermediate would be trapped by the addition of pyridine to provide **4**. Therefore, the isomerization of catalyst **8b** to **8a** was run in the presence of CuCl at 50 °C and monitored by ^{1}H NMR spectroscopy. When the isomerization had proceeded to above 50 %, pyridine (16 equivalents) was added and the reaction was stirred for 10 min at room temperature (Scheme 6). The complex was

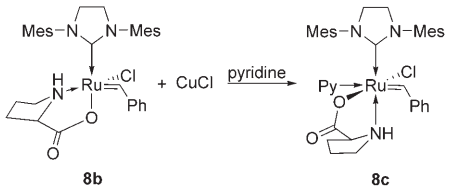

Scheme 6. Trapping intermediate with pyridine.

precipitated with pentane. The filtrate was separated and both the precipitate and the supernatant were analyzed by ^{1}H NMR spectroscopy. The ^{1}H NMR spectrum showed new signals in the aromatic region at δ 8.54, 6.68, and 6.66 ppm integrated to five protons. We assign these new peaks to one pyridine coordinated to ruthenium (Scheme 6, **8c**). Importantly, the aliphatic signals corresponding to prolinate are still present. The supernatant showed a weaker ^{1}H NMR spectrum with more pyridine present. Both samples were also analyzed by HRMS. As a control experiment, the same procedure was performed with catalyst **2** and complete conversion to **4** was observed.[5c] Furthermore, the supernatant only contained the Cy_3P–CuCl complex. This is strong support for path B (Scheme 5) where the prolinate ligand reversibly coordinates to CuCl. The κ^2-coordination mode of amino acids to CuCl is also strongly favored over the κ^1-coordination to the oxygen, which would be an intermediate in the salt exchange route, due to the softer nature of CuI.[16]

Conclusion

The synthesis of three catalysts featuring an L-type ligand tethered to a carboxylate replacing both a chloride ligand and a dative ligand catalyst **2** has been developed. Similar to other reported chelated ruthenium olefin metathesis catalysts, all three complexes show low catalytic activity in RCM at 30 °C. For the *N*,*O*- and the *P*,*O*-chelates **7** and **8**, respectively, this is likely due to a chelate effect and fast decomposition for the *O*,*O*-chelate **9**. The initiation for both *P*,*O*- and *N*,*O*-chelates can be improved by addition of CuCl with initial rates comparable to their non-chelated analogues. However, in the case of the *P*,*O*-chelate **7** the addition of CuCl does not lead to a more stable catalytic system, but rather a deviation from first-order kinetics is observed for more challenging substrates. Interestingly, in the case of *N*,*O*-chelate **8**, a very robust catalytic system is achieved when the cataly-

sis is run in the presence of CuCl with high efficiency in regards to initiation, reaction rate and stability. Trapping experiments support the hypothesis that the role of CuCl is to compete with ruthenium for the lone pair of the nitrogen thereby opening up a coordination site on ruthenium for the substrate.

Experimental Section

Synthesis of [(H_2IMES)(κ(*P,O*))(Ph_2P-*o*-C_6H_4COO)ClRu(CHPh)] (7): A Schlenk flask was charged with 2-(diphenylphosphino)benzoic acid (0.122 g, 0.4 mmol), KH (16 mg, 0.4 mmol) and THF (5 mL). The reaction was heated for 1 h at 50 °C, cooled to RT and solvents evaporated. [(NHC)(PCy_3)Cl_2Ru(CHPh)] (**2**) (340 mg, 0.4 mmol) and CH_2Cl_2 (5 mL) were added to the Schlenk flask. The reaction mixture was degassed by three pump-thaw cycles and the reaction was stirred for 5 h at RT. The reaction mixture was filtered through a glass-frit and concentrated in vacuo. The resulting solid was purified via column chromatography (TSI silica) using a gradient of diethyl ether and ethyl acetate to give **7** (250 mg, 75 %) as a red solid. ^{1}H NMR (300 MHz, C_6D_6): δ = 18.97 (s, 1H), 8.86 (m, 1H), 7.64 (m, 2H), 7.36 (m, 2H), 7.04 (m, 3H), 6.90 (m, 3H), 6.80 (m, 2H), 6.73 (m, 5H), 6.57 (m, 3H), 6.24 (s, 1H), 6.11 (s, 1H), 3.42 (m, 2H), 3.29 (m, 2H), 2.83 (s, 3H), 2.77 (s, 3H), 2.38 (s, 3H), 2.29 (s, 3H), 2.07 (s, 3H), 1.77 ppm (s, 3H); ^{13}C NMR (75 MHz, C_6D_6): δ = 300.2 (d, $J_{P,C}$ = 9.6 Hz), 220.0 (d, $J_{P,C}$ = 77.7 Hz), 170.0 (d, $J_{P,C}$ = 6.2 Hz), 127.6–151.4 (36 aromatic signals), 51.8, 51.0, 21.4, 20.9, 20.1, 19.4, 18.5, 18.22 ppm; ^{31}P NMR (121 MHz, C_6D_6): δ = 32.47 ppm; IR (CH_2Cl_2): $\tilde{\nu}$ = 3410, 3054, 2914, 1602 cm^{-1}; FAB-HRMS: *m/z*: calcd for $C_{47}H_{46}N_2O_2PRuCl$: 838.2051; found; 838.2029; elemental analysis calcd (%) for $C_{47}H_{46}N_2O_2PRuCl$: C 67.33, H 5.53, N 3.34; found: C 67.75, H 5.18, N 2.99.

Synthesis of [(H_2IMES)(Pro)ClRu(CHPh)] (8): A Schlenk flask was charged with [(NHC)(PCy_3)Cl_2Ru(CHPh)] (**2**) (220 mg, 0.26 mmol), L-proline (300 mg, 2.6 mmol), and Cu_2O (1 g, 6 mmol) and flushed with argon. CH_2Cl_2 (20 mL) was cannula transferred and the reaction was stirred for 5 h at RT under argon during which time a color change from red to green was observed. The reaction mixture was filtered through a glass-frit and concentrated in vacuo. The resulting solid was purified via column chromatography (TSI silica) using a gradient of ethyl acetate and MeOH to give **8** in two different fractions (37 mg and 53 mg) as a green solid in 54 % yield. Thermodynamically stable isomer **8a**: ^{1}H NMR (300 MHz, CD_2Cl_2): δ = 19.17 (s, 1H), 7.71 (m, 2H), 7.49 (m, 1H), 7.18 (m, 2H), 6.3–7.2 (m, 4H), 4.10 (m,4H), 3.54 (m, 1H), 1.6–2.9 (overlapping signals 22H), 1.43 ppm (m, 2H); ^{13}C NMR (75 MHz, CD_2Cl_2, −20 °C): δ = 296.3, 221.9, 183.2, 151.7, 124.8–141.2 (17 signals), 61.9, 51.8, 50.5, 45.2, 30.5, 24.5, 21.1, 20.9, 19.9, 18.8, 18.2, 17.9 ppm; IR (CH_2Cl_2): $\tilde{\nu}$ = 3462, 3054, 2914, 1602 cm^{-1}; FAB-HRMS: *m/z*: calcd for $C_{33}H_{40}N_3O_2ClRu$: 647.1866; found: 647.1853; elemental analysis calcd (%) for $C_{33}H_{40}N_3O_2ClRu$: C 61.24, H 6.23, N 6.41; found: C 62.16, H 6.12, N 6.02; kinetically formed isomer **8b**: ^{1}H NMR (300 MHz, CD_2Cl_2): δ = 19.03 (s, 1H), 7.77 (m, 2H), 7.47 (m, 1H), 7.18 (m, 2H), 7.07 (s, 1H), 7.04 (s, 1H), 6.53 (s, 1H), 6.21 (s, 1H), 4.10,(m, 2H), 4.08 (m, 2H), 2.95 (m, 1H), 2.79 (m, 1H), 2.63 (s, 3H), 2.40 (s, 3H), 2.37 (s, 3H), 2.15 (s, 3H), 2.05 (s, 3H), 2.02 (s, 3H), 1.2–2.2 ppm (overlapping signals 5H); ^{13}C NMR (75 MHz, CD_2Cl_2, −20 °C): δ = 297.3, 222.8, 185.2, 153.6, 130.6–143.2 (17 signals), 62.3, 53.7, 52.5, 47.3, 32.6, 23.5, 22.8, 22.1, 22.0, 20.2. 20.1, 19.9 ppm.

Synthesis of [(H_2IMES)(tetrahydrofuroiate)ClRu(CHPh)] (9): A Schlenk flask was charged with [(NHC)(PCy_3)Cl_2Ru(CHPh)] (**2**) (220 mg, 0.26 mmol), Ag_2O (60 mg, 0.26 mmol), and flushed with argon. CH_2Cl_2 (20 mL) was cannula transferred, (*R*)-(+)tetrahydro-2-furioc acid (90 μL, 2.6 mmol) was added via syringe and the reaction was stirred for 2 h at RT under argon during which time a color change from red to green was observed. The reaction mixture was filtered through a glass-frit and concentrated in vacuo. The resulting solid was purified via column chromatography (TSI silica) using a gradient of chloroform and MeOH to give **9** (129 mg) as a green solid in 81 % yield. Major isomer: ^{1}H NMR (300 MHz, CD_2Cl_2): δ = 19.00 (s, 1H), 7.71 (m, 2H), 7.54 (m, 2H), 7.24 (m, 2H), 6.80 (s, 4H), 3.98 (s, 4H), 3.92 (m, 1H), 3.59 (m, 2H), 2.27 (s, 6H), 2.23 (s, 6H), 2.19 (s, 6H), 1.94 (m, 2H), 1.69 ppm (m, 2H); ^{13}C NMR (75 MHz, CD_2Cl_2, −20 °C): δ = 315.6, 215.4, 179.7, 153.8, 138.5, 138.3, 129.7, 129.6, 129.6, 129.0, 128.9, 71.4, 69.7, 51.9, 29.6, 25.3, 25.2, 21.2, 18.5, 18.4 ppm; IR (CH_2Cl_2): $\tilde{\nu}$ = 3405, 2956, 2921, 1945, 1607 cm^{-1}; FAB-HRMS: *m/z*: calcd for $[C_{33}H_{39}N_2O_3Ru-HCl]^+$: 612.1926; found: 612.1925; elemental analysis calcd (%) for $C_{33}H_{40}N_2O_3ClRu$: C 61.05, H 6.21, N 4.32; found: C 60.4, H 6.00, N 3.46.

Acknowledgements

Financial support from the Swedish Research Council is gratefully acknowledged. We thank Drs D. R. Anderson, J. P. Jordan, and M. S. Malarek, for fruitful discussions. L. M. Henling and Dr M. W. Day are acknowledged for crystal structures of **7** and **8a**.

[1] *Handbook of Metathesis* (Ed.: R. H. Grubbs), Wiley-VCH, Weinheim, **2003**.
[2] T. M. Trnka, R. H. Grubbs, *Acc. Chem. Res.* **2001**, *34*, 18–29.
[3] M. Ulman, R. H. Grubbs, *J. Org. Chem.* **1999**, *64*, 7202–7207.
[4] S. H. Hong, D. P. Sanders, C. W. Lee, R. H. Grubbs, *J. Am. Chem. Soc.* **2005**, *127*, 17160–17161.
[5] a) M. Scholl, S. Ding, C. W. Lee, R. H. Grubbs, *Org. Lett.* **1999**, *1*, 953–956; b) S. B. Garber, J. S. Kingsbury, B. L. Gray, A. H. Hoveyda, *J. Am. Chem. Soc.* **2000**, *122*, 8168–8179; c) S. Gessler, S. Randl, S. Blechert, *Tetrahedron Lett.* **2000**, *41*, 9973–9976; d) M. S. Sanford, J. A. Love, R. H. Grubbs, *Organometallics* **2001**, *20*, 5314–5318.
[6] a) S. H. Hong, M. W. Day, R. H. Grubbs, *J. Am. Chem. Soc.* **2004**, *126*, 7414–7415; b) S. H. Hong, A. G. Wenzel, T. T. Salguero, M. W. Day, R. H. Grubbs, *J. Am. Chem. Soc.* **2007**, *129*, 7961–7968.
[7] a) K. Denk, J. Fridgen, W. Herrmann, *Adv. Synth. Catal.* **2002**, *344*, 666–670; b) B. Allaert, N. Dielliens, N. Ledoux, C. Vercaemst, P. Van Der Voort, C. V. Stevens, A. Linden, F. Verpoort, *J. Mol. Catal. A* **2006**, *260*, 5482–5486; c) J. B. Binder, I. A. Guzei, R. T. Raines, *Adv. Synth. Catal.* **2007**, *349*, 395–404; d) M. Jordaan, H. C. M. Vosloo, *Adv. Synth. Catal.* **2007**, *349*, 184–192.
[8] The Verpoort group has earlier reported a less toxic protocol for the bidentate Schiff base ligands. Unfortunately, different groups, including our group and also their own group, have had difficulties reproducing their data.
[9] J. S. M. Samec, R. H. Grubbs, *Chem. Commun.* **2007**, 2826–2828.
[10] Other groups have also observed an rate enhancement when the X-type ligand is changed from an alkoxide to a carboxylate, see; T. S. Halbach, S. Mix, D. Fischer, S. Maechling, J. O. Krause, C. Sievers, S. Blechert, O. Nuyken, M. R. Buchmeiser, *J. Org. Chem.* **2005**, *70*, 4687–4694. For other reports on using carboxylates as X-type ligands, see; R. Gawin, A. Makal, K. Wozniak, M. Mauduit, K. Grela, *Angew. Chem.* **2007**, *119*, 7344–7347; *Angew. Chem. Int. Ed.* **2007**, *46*, 7206–7209 and J. O. Krause, O. Nuyken, K. Wurst, M. R. Buchmeister, *Chem. Eur. J.* **2004**, *10*, 777–784.
[11] J. A. Love, M. S. Sanford, M. W. Day, R. H. Grubbs, *J. Am. Chem. Soc.* **2003**, *125*, 10103–10109.
[12] T. Ung, A. Hejl, R. H. Grubbs, Y. Schrodi, *Organometallics* **2004**, *23*, 5399–5401.
[13] The thermodynamically more stable isomer was used in the kinetics.
[14] T. Ritter, A. Hejl, A. G. Wenzel, T. W. Funk, R. H. Grubbs, *Organometallics* **2006**, *25*, 5740–5745.
[15] a) E. L. Dias, S. T. Nguyen, R. H. Grubbs, *J. Am. Chem. Soc.* **1997**, *119*, 3887–3897; b) J. P. Morgan, R. H. Grubbs, *Org. Lett.* **2000**, *2*, 3153–3155.
[16] a) B. A. Cerda, C. Wesdemiotis, *J. Am. Chem. Soc.* **1995**, *117*, 9734–9739; b) J. Bertran, L. Rodriguez-Santiago, M. Sodupe, *J. Phys.*

Chem. B **1999**, *103*, 2310–2317; c) A. Rimola, L. Rodriguez-Santiago, M. Sodupe, *J. Phys. Chem. B* **2006**, *110*, 24189–24199.

[17] Such salt exchange routes have been reported, see: C. Wallenhorst, K. V. Axenov, G. Kehr, J. S. M. Samec, R. Fröhlich, G. Erker, *Z. Naturforsch. B* **2007**, *62*, 783–790.

Received: September 21, 2007
Published online: January 31, 2008

